processes

MDPI

*Article*

# Evaluation of Process Control Schemes for Sour Water Strippers in Petroleum Refining

**Chii-Dong Ho, Yih-Hang Chen *, Chao-Min Chang and Hsuan Chang**

Department of Chemical and Materials Engineering, Tamkang University, New Taipei City 25137, Taiwan; cdho@mail.tku.edu.tw (C.-D.H.); popo3989500@gmail.com (C.-M.C.); nhchang@mail.tku.edu.tw (H.C.)
* Correspondence: yihhang@mail.tku.edu.tw

**Abstract:** For the sour water strippers in petroleum refinery plants, three prediction models were developed first, including the estimators of sour water feed concentrations using convenient online measurements, the minimum reboiler duty and the corresponding internal temperature at a specific location ($T_{stage,29}$). Feedforward control schemes were developed based on these prediction models. Four categories of control schemes, including feedforward, feedback, feedback with external reset, and feedforward-feedback, were proposed and evaluated by the rigorous dynamic simulation model of the sour water stripper for their dynamic responses to the sour water feed stream disturbances. The comparison of control performance, in terms of the settling time, integrated absolute error (IAE) of the $NH_3$ concentration of the stripped sour water and IAE of the specific reboiler duty, reveals that FFT (feedforward control of $T_{stage,29}$) and FBA-DT3 (feedback control with 3 min concentration measurement delay) are the best control schemes. The second-best control scheme is FBAT (cascade feedback control of concentration with temperature).

**Keywords:** sour water; stripping; process control; soft sensors



**Citation:** Ho, C.-D.; Chen, Y.-H.; Chang, C.-M.; Chang, H. Evaluation of Process Control Schemes for Sour Water Strippers in Petroleum Refining. *Processes* **2021**, *9*, 363. https://doi.org/10.3390/pr9020363

Academic Editor: Matti Lehtonen

Received: 16 January 2021
Accepted: 11 February 2021
Published: 16 February 2021



## 1. Introduction

Even with extensive recycling and reuse of process water, petroleum refining industry still consumes 0.34–0.47 L makeup water/L crude [1]. In oil refineries, steam and/or water is used in various refinery units, such as delayed cokers, hydrotreaters, hydrocrackers, fluidized catalytic cracker (FCCU), and visbreaker fractionators. The effluent from those process units is the sour water contaminated by phenol, ammonia ($NH_3$), hydrogen sulfide ($H_2S$), and possibly trace of carbon dioxide ($CO_2$). The phenolic sour water is generated from FCCU, whereas the nonphenolic sour water is generated from process units other than the FCCU. The phenolic sour water cannot be recycled back for reuse as it is harmful to the catalysts [2]. Nonphenolic sour water can be treated and reused as the wash water for the crude desalter or the make-up to the hydrotreater effluent wash water. Treated sour water for these reuses is demanded to meet stringent quality, i.e., the $NH_3$ content must be lower than 10–20 ppmw and a few hundred ppmw, respectively [3,4]. Treated sour water which cannot comply with the specifications for reuse must be diverted to the effluent water treatment plant. That will hence cause the increase of both freshwater consumption and wastewater emission.

A stripper with an externally heated reboiler is the most employed configuration for sour water treatment in petroleum refining. Aiming for energy saving, one approach is to develop alternative sour water stripping configurations, such as split flow and vapor recompression [5–7]. Another approach is to keep tight operation of the sour water stripper (SWS) which consumes minimal amount of steam while meeting the concentration limit of the stripped sour water (SSW). One of the practical operating problems involved in the sour water stripping process is the variable feed flowrate and composition due to multiple sour water sources, as each source has a different flowrate and contains varying concentrations of $H_2S$ and $NH_3$ [8]. Even with long-time (three- to five-day) storage for stabilizing the

composition of the feed to the stripper, tight operation of SWS is a challenging task because of the lack of online composition measurements for feed and SSW streams and the guideline for minimum energy operation.

Development of soft sensors is an approach to deal with the online measurement problem. A deep learning neural network model was developed by Graziani and Xibilia [9] to function as the soft sensors of the $H_2S$ and $NH_3$ concentrations for the SSW. The data-driven model was developed based on historical plant operating data and employed the stripper feed flowrate, pressure, temperature, and steam flowrate as inputs. Another data-driven soft sensor was reported by Barros et al. [10] for estimating the $H_2S$ removal efficiency for a two-column sour water stripping process. To the knowledge of the authors of this paper, very few studies have been focused on the process control of SWS. The control system of SWS illustrated in the literature consists of only basic inventory control loops, such as the column pressure, liquid level, and flow control [2,8,11]. The quality control commonly adopted is the ratio control, which keeps a fixed ratio of steam flowrate to sour water feed flowrate [2]. Morado et al. [12] developed a response surface model to determine the ratio to respond for the disturbance of sour water feed flowrate for a two-stage sour water stripping process. However, the composition of the sour water feed was fixed in the study.

This study aims to develop prediction models and process control schemes for the SWS operation to respond to the feed disturbances with the compliance of the SSW concentration limit using minimum amount of energy. The prediction models include the soft sensor models for feed composition estimation and the correlations for the minimum reboiler duty and the corresponding internal temperature at a specific location of the stripper. The control schemes proposed include feedforward, feedback, feedback with external reset, and feedforward-feedback configurations. In this paper, the design and simulation model for SWS as well as the prediction models are explained first. Secondly, the proposed control schemes are illustrated. Finally, the dynamic responses and the control performance of the control schemes to the feed disturbances are presented and compared.

## 2. Process Simulation and Prediction Model Development

### 2.1. Steady and Dynamic Simulation

The industrial scale SWS studied in this paper is shown in Figure 1. The base case operation conditions and column size specifications are also depicted in the figure. The pump-around cooling design can reduce both the water entrainment of the overhead vapor and the plugging and corrosion potential [8]. The reboiler heated by steam provides the energy to strip off the $NH_3$ and $H_2S$ from the sour water feed stream. The water-washing section employs Pall ring type packing to enhance heat transfer, while the stripping section uses sieve tray to prevent fouling and plugging.

The steady state and dynamic simulations of the SWS utilized the Radfrac unit of Aspen Plus® and Aspen Plus Dynamics® [13], respectively. The thermodynamic model used is ELECNRTL with the specification of $NH_3$ and $H_2S$ as Henry's components. The vapor-liquid equilibria of aqueous solution of $NH_3$ and $H_2S$ was verified with the experimental data from Newman [14].

The rate-based model of Radfrac, which takes into account the heat and mass transfer rates, was adopted for the steady state simulation. However, to reduce the computational load and the converging difficulty, the dynamic simulation adopted the equilibrium model of Radfrac with the Murphree efficiencies of $NH_3$ and $H_2S$ determined from the steady state rate-based simulation.

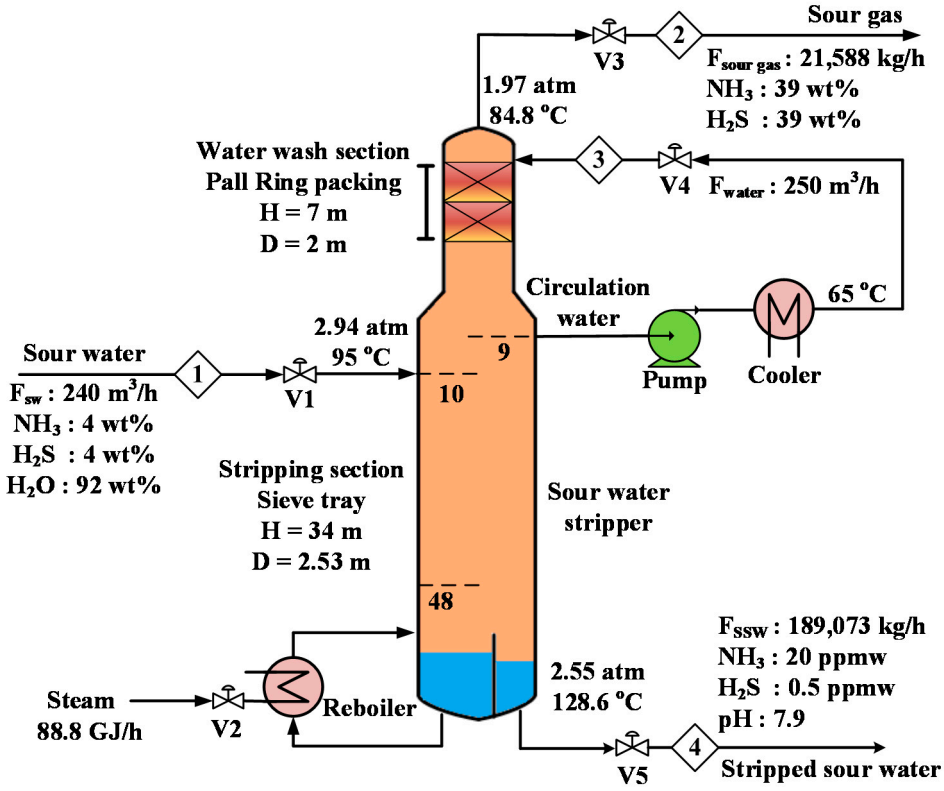


**Figure 1.** A sour water stripper with column specifications and base case operation conditions.

### *2.2. Feed Composition Estimator*

Feed composition analysis is normally not implemented in real plant operation or takes a significant amount of time to obtain the laboratory test data. It is hence impossible to take prompt dynamic control actions for feed composition disturbances. Unlike composition, liquid density, pH and temperature of the feed stream can be online measured conveniently. An estimation model for feed composition using these easily measured properties of sour water feed stream could significantly improve the dynamic operation of SWS.

For the sour water fed to the SWS, two composition estimation models were developed based on the simulation data using ELECNRTL thermodynamic model. The effects of sour water composition and temperature on the mass density and pH value are shown in Figure 2. For the mass fractions of $H_2S$ and $NH_3$ of the sour water feed stream, the quadratic polynomial functions obtained by regression are:

$$X_{SW,H_2S} = 336.59 - 0.63T_{SW} - 0.47\varrho_{SW} - 15.65pH_{SW} + 0.00081T_{SW}\varrho_{SW} - 0.021T_{SW}pH_{SW} + 0.0314\varrho_{SW}pH_{SW} + 5.28 \times 10^{-5}\varrho_{SW}^2 - 0.789pH_{SW}^2 \quad (1)$$

$$X_{SW,NH_3} = -224.79 + 0.71T_{SW} + 0.28\varrho_{SW} + 20.5pH_{SW} - 0.00063T_{SW}\varrho_{SW} - 0.04\varrho_{SW}pH_{SW} - 0.00075T_{SW}^2 + 2.43 \times 10^{-5}\varrho_{SW}^2 + 1.14\,pH_{SW}^2 \quad (2)$$

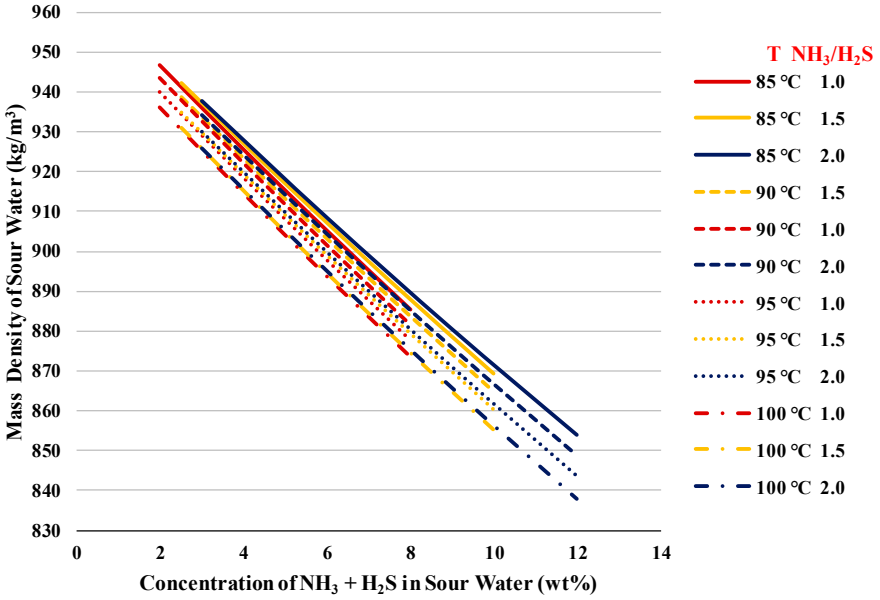


(**a**) mass density

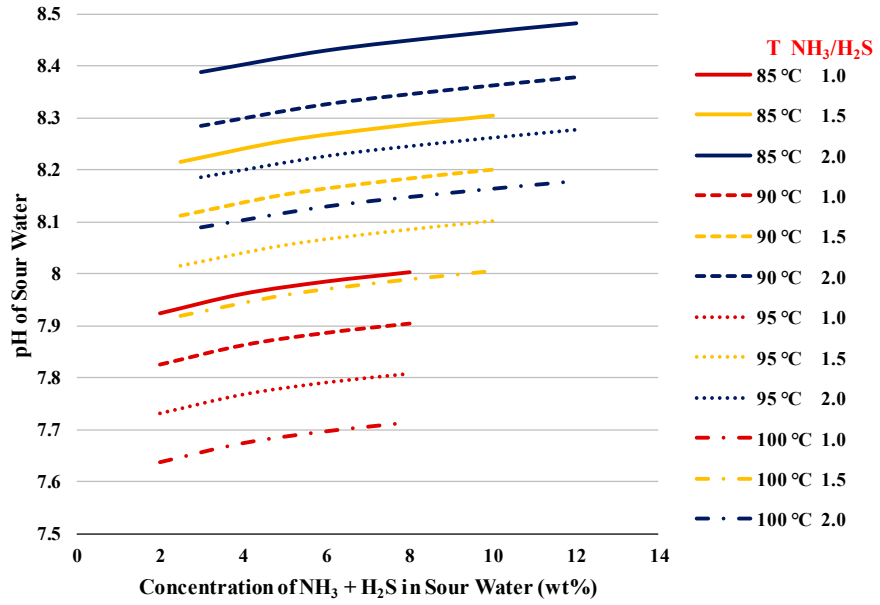


(**b**) pH

**Figure 2.** Effects of temperature and concentrations of $NH_3$ and $H_2S$ on the sour water properties.

The right-hand-side terms of Equations (1) and (2) are statistically significant judged via the probability $p$-value < 0.05. The coefficients of determination ($R^2$) of both models are higher than 0.99.

### *2.3. Minimum Reboiler Duty Predictor*

The goal of SWS operation is to comply with the $NH_3$ concentration limit of the SSW using minimum reboiler duty. As the feed stream composition, which is difficult to measure online, can be estimated using Equations (1) and (2), a predictor for the minimum reboiler duty required can guide the operation and control.

Response surface methodology (RSM) explores the relationships between several explanatory variables and one or more of response variables. The relationships are expressed by second-degree polynomial models. RSM uses a sequence of designed experiments to

obtain an optimal response, i.e., a best-fit of the experimental data to the model. Note that in this study, the experimental data are the results from Aspen Plus® simulation instead of the plant operation data. By applying the experimental design method of central composite design [15] for four factors, 25 simulation cases (Table 1) were determined. The considered sour water feed conditions are flowrate of 120–300 $m^3/h$, temperature of 85–100 °C, $H_2S$ concentration of 1–4 wt%, and mass ratio of $NH_3$ to $H_2S$ of 1–2. For each case, the minimum reboiler duty required to achieve the bottom $NH_3$ concentration of 20 ppmw was obtained from the steady state SWS simulation using Aspen Plus®. The second-degree polynomial model for the minimum reboiler duty determined has a $R^2$ of 0.999. The model parameters are statistically significant with *p*-values less than 0.05 (Table 2). The predictor model expressed in terms of the minimum reboiler duty per unit sour water feed flowrate is:

$$\begin{aligned} Q_R/F_{SW} &= 0.47 - 1.3 \times 10^{-4}F_{SW} + 7.6 \times 10^{-3}X_{SW,H_2S} + 2.8 \times 10^{-2}X_{SW,NH_3} - 1.7 \times 10^{-3}T_{SW} \\ &+ 5.1 \times 10^{-6}F_{SW}X_{SW,H_2S} + 2.1 \times 10^{-6}F_{SW}X_{SW,NH_3} - 4.3 \times 10^{-7}F_{SW}T_{SW} - 9.4 \times 10^{-5}T_{SW}X_{SW,NH_3} + 1.8 \times 10^{-7}F_{SW}^2 \\ &- 4.9 \times 10^{-4}T_{SW}^2 - 8.9 \times 10^{-4}X_{SW,H_2S}^2 - 5 \times 10^{-4}X_{SW,NH_3}^2 \end{aligned} \quad (3)$$

**Table 1.** Experimental simulation cases for the development of minimum reboiler duty predictor.

| Case | $F_{SW}$ ($m^3/h$) | $X_{SW,H_2S}$ (wt%) | $X_{SW,NH_3}/X_{SW,H_2S}$ | T (°C) | Case | $F_{SW}$ ($m^3/h$) | $X_{SW,H_2S}$ (wt%) | $X_{SW,NH_3}/X_{SW,H_2S}$ | T (°C) |
|---|---|---|---|---|---|---|---|---|---|
| 1 | 165 | 2.5 | 1.25 | 85 | 14 | 255 | 3.5 | 1.25 | 95 |
| 2 | 165 | 2.5 | 1.25 | 95 | 15 | 255 | 3.5 | 1.75 | 85 |
| 3 | 165 | 2.5 | 1.75 | 85 | 16 | 255 | 3.5 | 1.75 | 95 |
| 4 | 165 | 2.5 | 1.75 | 95 | 17 | 120 | 3 | 1.5 | 90 |
| 5 | 165 | 3.5 | 1.25 | 85 | 18 | 300 | 3 | 1.5 | 90 |
| 6 | 165 | 3.5 | 1.25 | 95 | 19 | 210 | 2 | 1.5 | 90 |
| 7 | 165 | 3.5 | 1.75 | 85 | 20 | 210 | 4 | 1.5 | 90 |
| 8 | 165 | 3.5 | 1.75 | 95 | 21 | 210 | 3 | 1 | 90 |
| 9 | 255 | 2.5 | 1.25 | 85 | 22 | 210 | 3 | 2 | 90 |
| 10 | 255 | 2.5 | 1.25 | 95 | 23 | 210 | 3 | 1.5 | 80 |
| 11 | 255 | 2.5 | 1.75 | 85 | 24 | 210 | 3 | 1.5 | 100 |
| 12 | 255 | 2.5 | 1.75 | 95 | 25 | 210 | 3 | 1.5 | 90 |
| 13 | 255 | 3.5 | 1.25 | 85 | | | | | |

**Table 2.** The parameters of the minimum reboiler duty predictor.

| Parameter | Value | *p*-Value | Parameter | Value | *p*-Value |
|---|---|---|---|---|---|
| Constant | $4.7 \times 10^{-1}$ | $2.65 \times 10^{-15}$ | $F_{SW}T_{SW}$ | $-4.3 \times 10^{-7}$ | 0.023 |
| $F_{SW}$ | $-1.3 \times 10^{-4}$ | 0.002 | $T_{SW}X_{SW,NH_3}$ | $-9.4 \times 10^{-5}$ | $2.61 \times 10^{-5}$ |
| $X_{SW,H_2S}$ | $7.6 \times 10^{-3}$ | 0.001 | $F_{SW}^2$ | $1.8 \times 10^{-7}$ | $1.0 \times 10^{-3}$ |
| $X_{SW,NH_3}$ | $2.8 \times 10^{-2}$ | $2.36 \times 10^{-10}$ | $T_{SW}^2$ | $-4.9 \times 10^{-4}$ | $2.53 \times 10^{-8}$ |
| $T_{SW}$ | $-1.7 \times 10^{-3}$ | $5.45 \times 10^{-10}$ | $X_{SW,H_2S}^2$ | $-5.0 \times 10^{-4}$ | $7.18 \times 10^{-5}$ |
| $F_{SW}X_{SW,H_2S}$ | $5.1 \times 10^{-6}$ | 0.03 | $X_{SW,NH_3}^2$ | $-8.9 \times 10^{-4}$ | $4.19 \times 10^{-9}$ |
| $F_{SW}X_{SW,NH_3}$ | $2.1 \times 10^{-6}$ | 0.005 | | | |

### *2.4. Minimum Reboiler Duty Tray Temperature Predictor*

Inferential control [16] using temperature of a specific internal location, which is more sensitive to the control action, is common for separation columns. Sensitivity analysis can be conducted by varying the reboiler duty to obtain its effect on the temperature of each stage of the SWS, as shown in Figure 3. The most sensitive location is stage 29. Its temperature corresponding to the minimum reboiler duty can be used as the setpoint value of the temperature controller. For this purpose, a model was developed to predict the temperature of stage 29 under the minimum reboiler duty operation for different sour water feed conditions. The RSM explained in Section 2.3 was employed to obtain the following predictor:

$$T_{stage,29} = 9.6 \times 10^{-3} + 2.93 \times 10^{-5}F_{SW} - 2.5 \times 10^{-3}X_{SW,H_2S} - 1.4 \times 10^{-3}X_{SW,NH_3} - 4.89 \times 10^{-5}T_{SW} - 2.38 \times 10^{-6}F_{SW}X_{SW,H_2S} - 1.44 \times 10^{-6}F_{SW}X_{SW,NH_3} - 9.17 \times 10^{-8}F_{SW}T_{SW} - 1.28 \times 10^{-4}X_{SW,NH_3}X_{SW,H_2S} - 8.97 \times 10^{-6}X_{SW,H_2S}T_{SW} + 3.97 \times 10^{-6}X_{SW,NH_3}T_{SW} + 1.81 \times 10^{-4}X^2_{SW,NH_3} - 2.71 \times 10^{-4}X^2_{SW,H_2S} \quad (4)$$

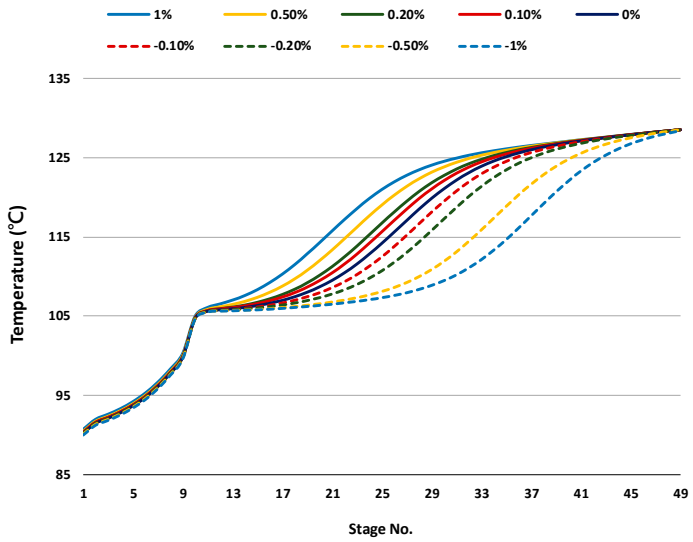


**Figure 3.** Sensitivity of stage temperature on percent variation of reboiler duty.

The $R^2$ of the model is greater than 0.99. All the model parameters are of statistical significance with $p$-value < 0.05.

## 3. Control Schemes

For the control of SWS to meet the $NH_3$ concentration target of the SSW, in addition to the traditional feedback control scheme, several feedforward and feedforward-feedback control schemes can be developed for the disturbances from the sour water feed stream utilizing the prediction models presented in Section 2. The block diagram of the three control types is shown in Figure 4. This section presents the details of the proposed control schemes.

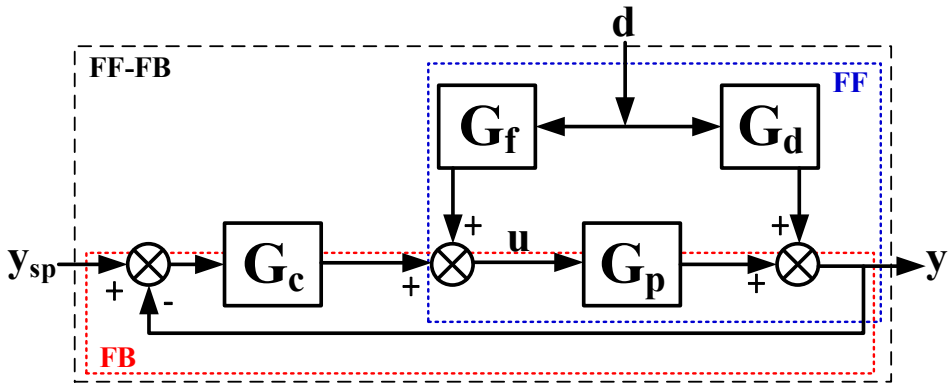


**Figure 4.** Block diagram for feedforward (FF) control, feedback (FB) control and feedforward-feedback (FF-FB) control. (d: disturbance, $y_{sp}$: set point of controlled variable, y: controlled variable, u: manipulated variable, $G_p$: process transfer function, $G_c$: feedback controller transfer function, $G_d$: disturbance transfer function, $G_f$: feedforward controller transfer function).

All the control schemes discussed employ the same inventory control loops, which include the control of column top pressure, washing water flowrate, and the column bottom

liquid level using PI, PID, and P control, respectively. The controller parameters suggested by Luyben [17] were adopted. These control loops are shown in Figures 5–7.

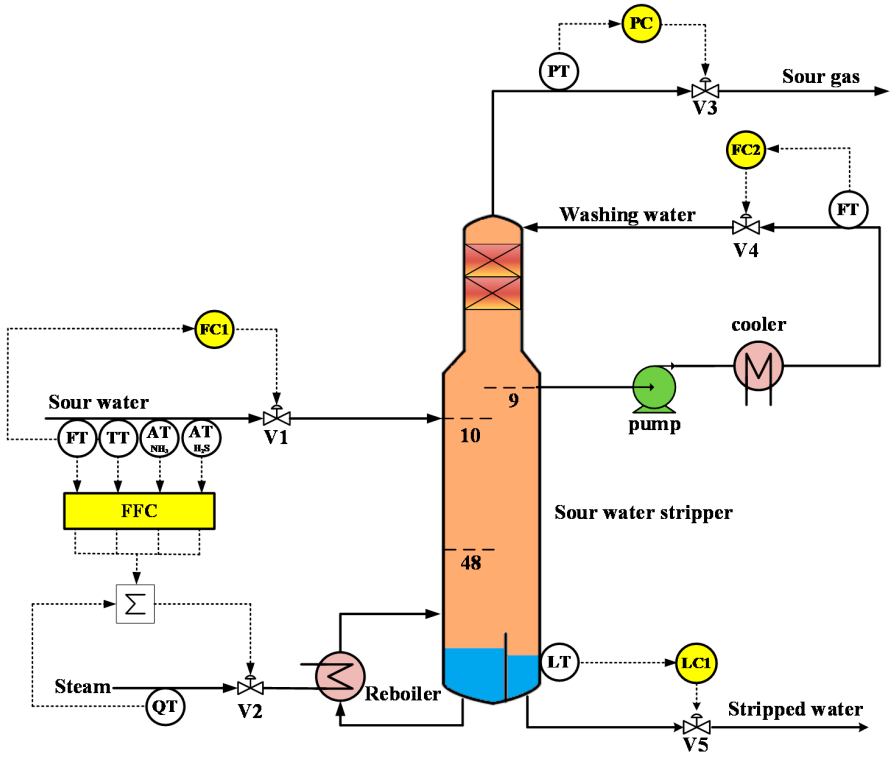


(**a**) FFQ-1

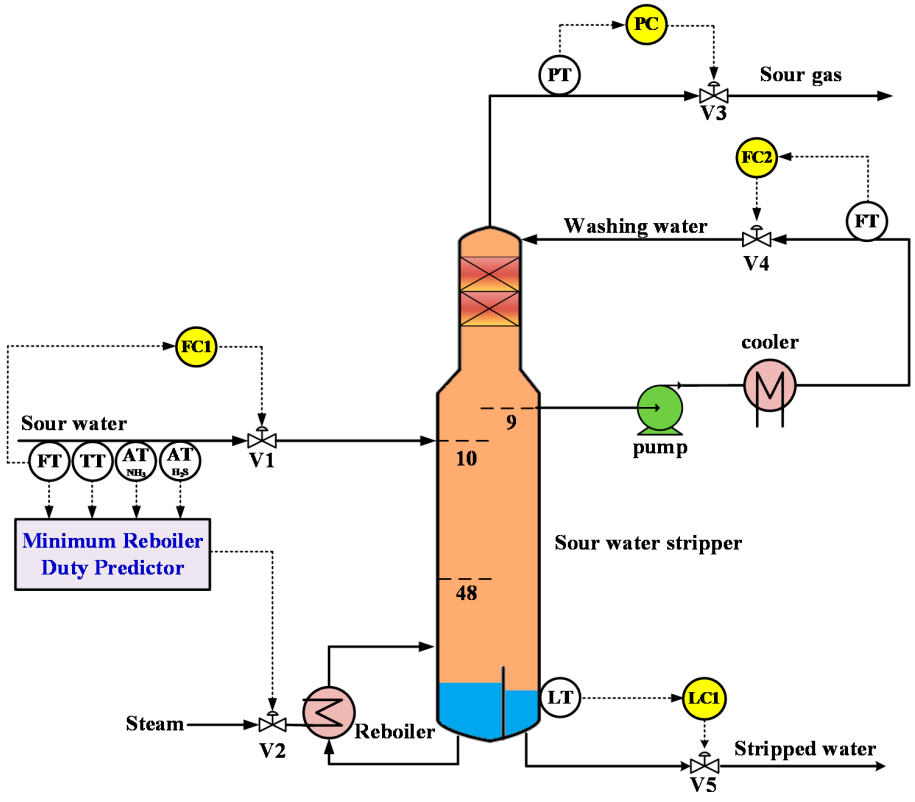


(**b**) FFQ-2

**Figure 5.** *Cont.*

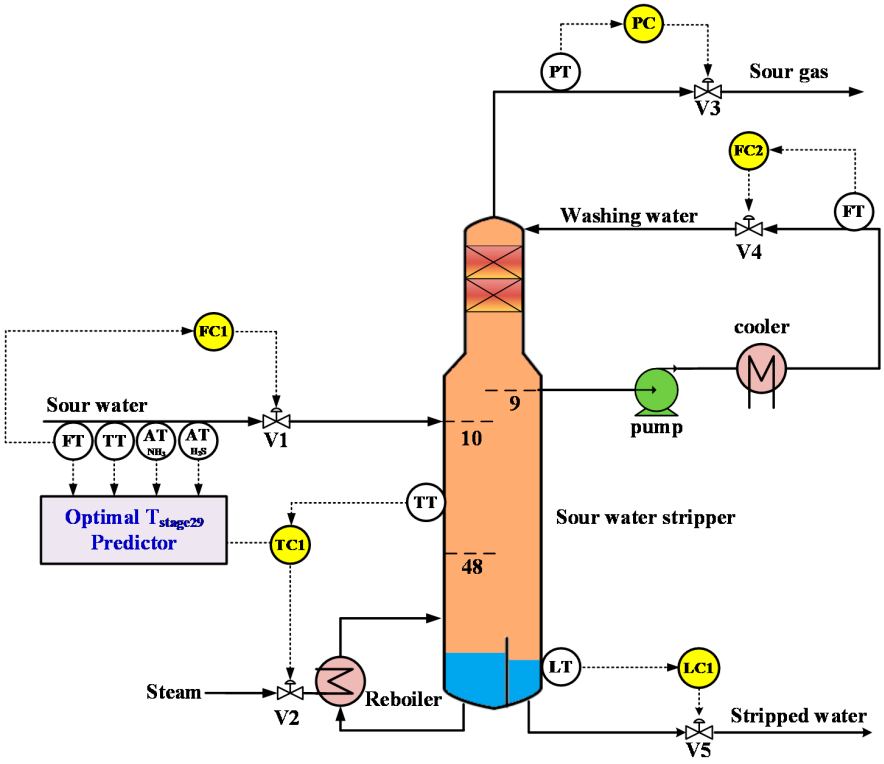


(**c**) FFT

**Figure 5.** Feedforward control schemes.

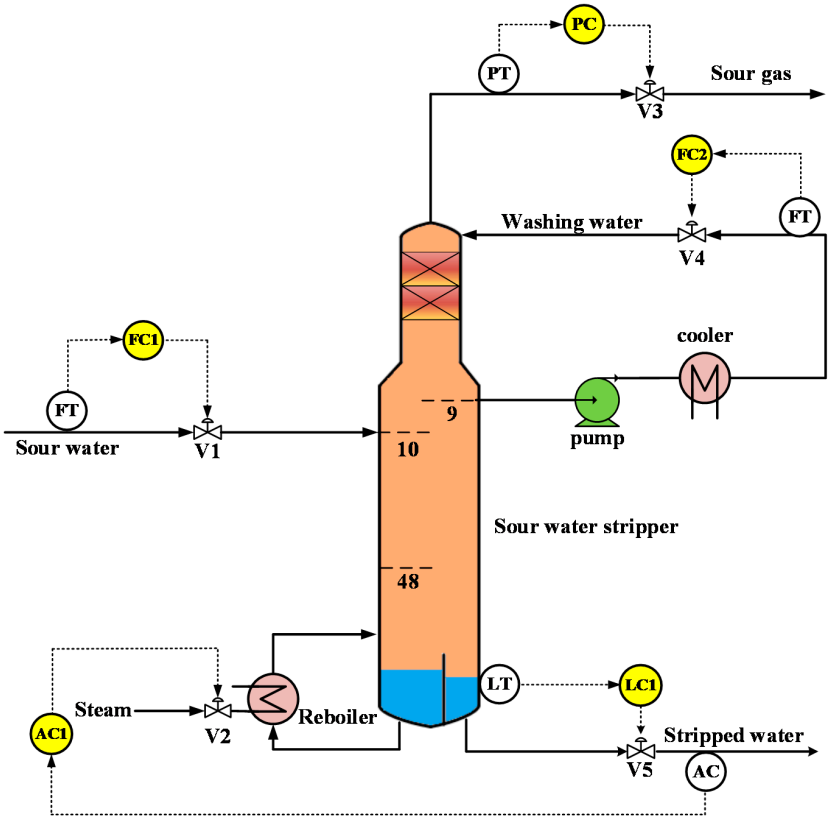


(**a**) FBA-DT

**Figure 6.** *Cont.*

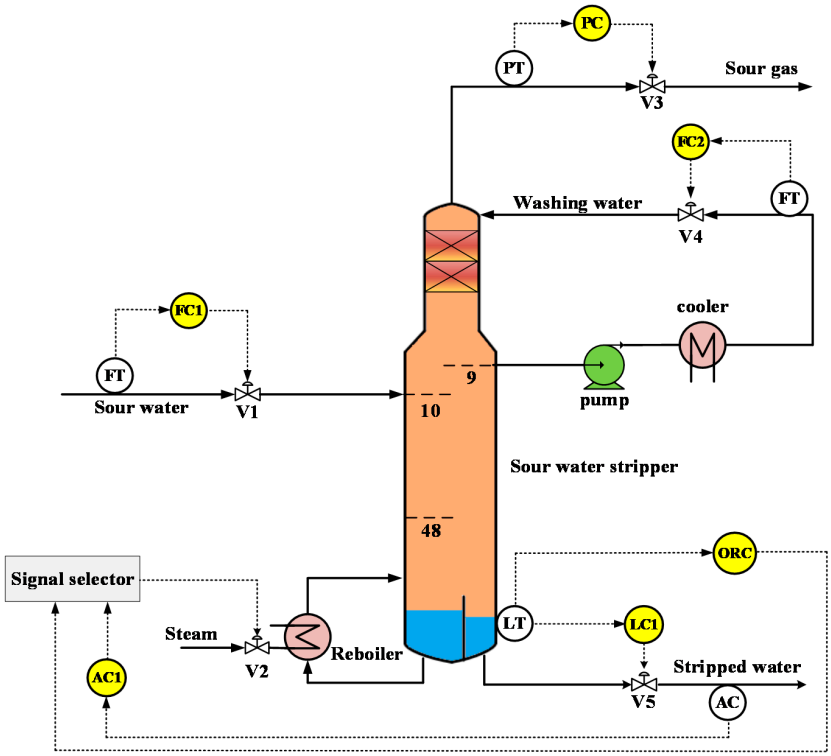


(**b**) FB-ER

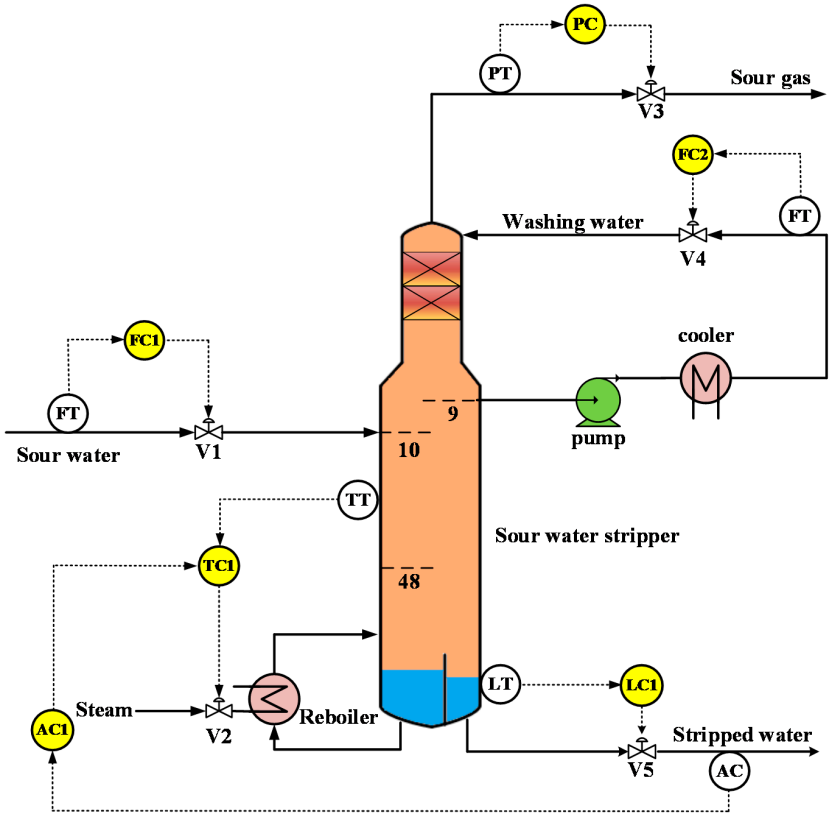


(**c**) FBAT

**Figure 6.** Feedback control schemes.

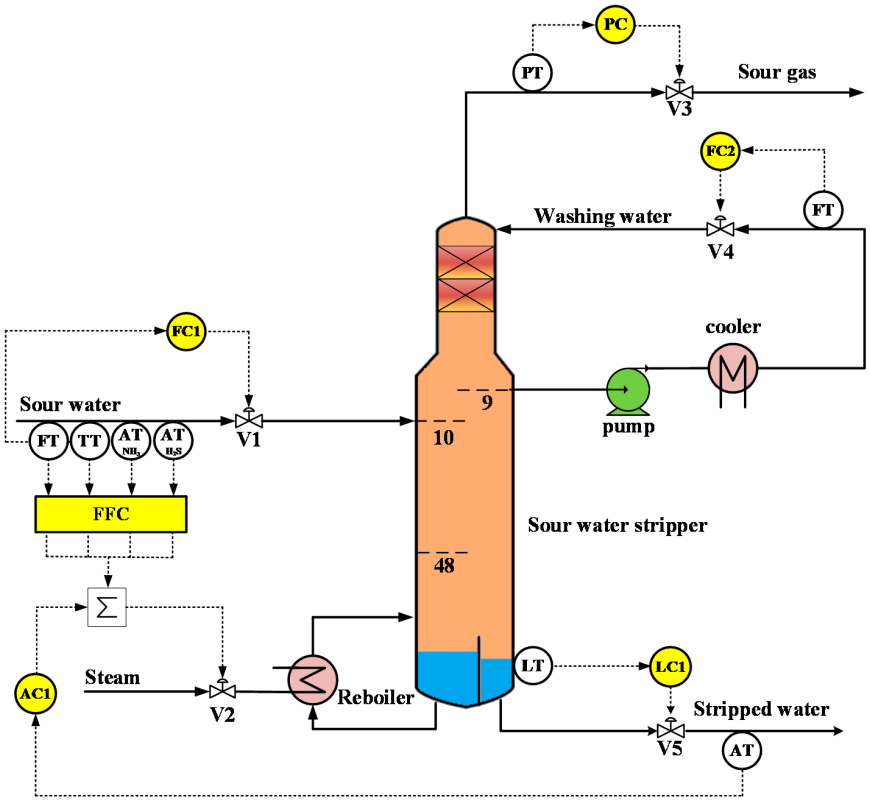


(**a**) FFQ-1-FBA

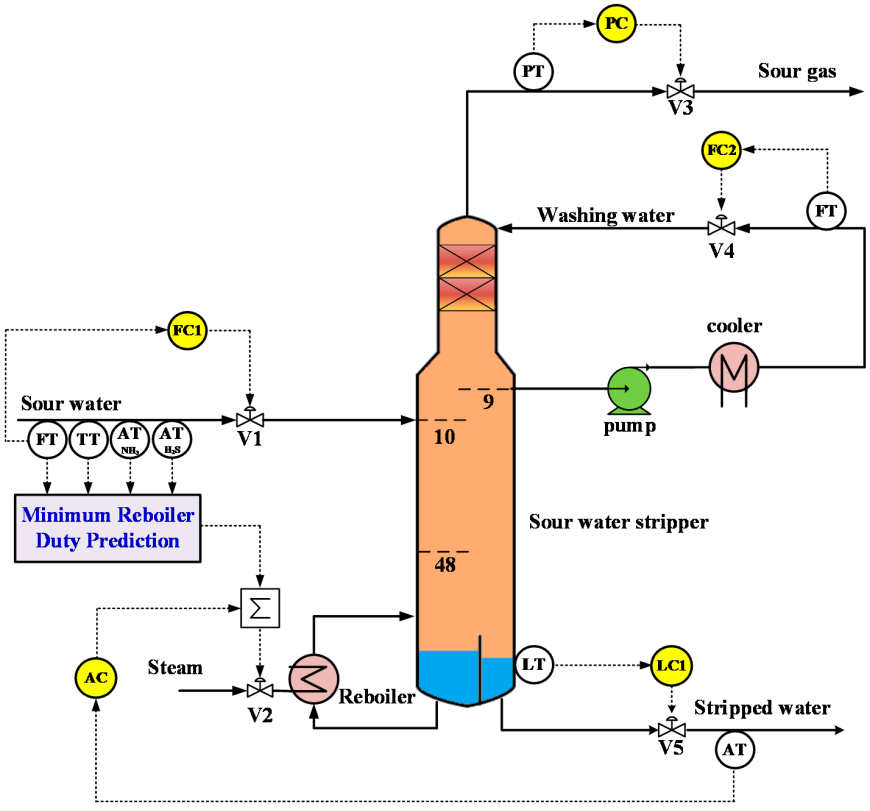


(**b**) FFQ-2-FBA

**Figure 7.** Feedforward-feedback control schemes.

### *3.1. Feedforward Control*

The feedforward control schemes proposed are depicted in Figure 5 and named FFQ-1, FFQ-2, and FFT. The first scheme is based on dynamic process models, and the latter two schemes are based on the steady state prediction models described in Sections 2.3 and 2.4. As soon as the changes of feed sour water conditions are detected, the first scheme provides dynamic compensation to the effects on the SWS, whereas the latter two schemes set the appropriate controllers to the optimal values for minimum reboiler duty operation.

In FFQ-1, as shown in Figure 5a, an ideal transfer function $G_f$ was used to compensate the effect of disturbance d. By assuming $G_p$ and $G_d$ both are first-order-plus-dead-time (FOPDT), $G_f$ is a lead-lag unit with a gain plus dead time:

$$G_f = K_f\left(\frac{\beta s+1}{\alpha s+1}\right)e^{-\theta_f} = -\frac{G_d}{G_p} = -\left(\frac{K_d}{K_p}\right)\left(\frac{\tau_p s+1}{\tau_d s+1}\right)e^{-(\theta_d-\theta_p)} \quad (5)$$

The parameters of $G_p$ and $G_d$, i.e., K, $\tau$ and $\theta$, were determined by open-loop testing using the dynamic simulation model of SWS for the operations at both high and low $NH_3$ concentration levels of SSW. The concentration levels are about 13,000 and 20 ppmw. The parameters of Equation (5) obtained for both concentration levels were averaged to obtain the transfer function for control performance evaluation. The averaged parameters for each of the sour water feed stream disturbance are listed in Table 3.

**Table 3.** Parameters of feedforward controller transfer functions for sour water feed stream disturbances.

| Disturbance | $K_f$ (%/%) | $\alpha$ (h) | $\beta$ (h) | $\theta_f$ (h) |
|---|---|---|---|---|
| $F_{SW}$ | 0.849 | 3.795 | 3.72 | 0.068 |
| $T_{SW}$ | 0.103 | 3.773 | 3.72 | 0.084 |
| $X_{SW,NH_3}$ | 0.257 | 0.782 | 3.72 | 0.360 |
| $X_{SW,H_2S}$ | 0.122 | 1.268 | 3.72 | 0.450 |

In FFQ-2, as shown in Figure 5b, the minimum reboiler duty is calculated with the measured sour water feed stream conditions, including flow flowrate, temperature, mass density, and pH value, using the model given in Equation (3). The minimum reboiler duty is then used as the setpoint of the heat duty controller, which is controlled by manipulating steam flowrate.

In FFT, as shown in Figure 5c, for the measured sour water feed stream conditions, including flow rate, temperature, mass density, and pH value, the temperature of stage 29 corresponding to the minimum reboiler duty operation is calculated using Equation (4). The temperature is then used as the setpoint of the temperature controller for stage 29.

### *3.2. Feedback Control*

The first feedback control scheme of SWS is the control loop using the $NH_3$ concentration of SSW and the reboiler duty as the controlled variable and the manipulated variable, respectively. This basic scheme, named FB-DT, is shown in Figure 6a and the time delays of 3, 10, and 20 min for composition measurement were considered. The closed-loop Ziegler–Nichols method [18] was utilized for the tuning of the composition controller.

As FB-DT experiences the integration windup problem, which occurs when a feedback controller with integral action cannot drive the process variable to the setpoint, a revised control scheme employing the override control structure with external reset feedback [19,20], as shown in Figure 6b and named as FB-ER, was devised. The column bottom liquid level controller was chosen as the override controller (ORC). The controller output signals from ORC and composition controller are compared in a lower-selector unit and the lower one goes to the control valve.

The third feedback control scheme is a cascade structure where the output of the composition controller is used to adjust the setpoint of the temperature controller of stage 29. The control scheme is called FBAT and shown in Figure 6c.

### *3.3. Feedforward-Feedback Control*

The purpose of employing feedforward-feedback control schemes is to improve both the feedforward and feedback parts. For the feedforward control, FFQ-1 and FFQ-2 were chosen because of the steady state offset in their dynamic responses, which will be presented in Section 4.1. Whereas, for the feedback control, the FBA-DT with the longest concentration measurement delay, i.e., 20 min, was chosen. The control schemes of FFQ-1-FBA and FFQ-2-FBA are shown in Figure 7.

## 4. Performance of Control Schemes

### *4.1. Dynamic Responses*

For all the control schemes, the dynamic responses to the disturbances of sour water feed stream, including ±10% change of flow flowrate, temperature, $NH_3$ concentration, and $H_2S$ concentration, were simulated using Aspen Plus Dynamics®. Note that with the sour water feed stream concentration estimation models developed for $NH_3$ and $H_2S$ as presented in Section 2.2, the disturbances of sour water feed stream can be detected instantly.

For the flow rate disturbance with −10% change and the $NH_3$ concentration disturbance with +10% change, the responses of reboiler duty ($Q_R$) and $NH_3$ concentration of the SSW ($X_{SSW,NH_3}$) are summarized in Figures 8 and 9, respectively.

The responses of feedforward control schemes to −10% feed flowrate change are shown in Figure 8a,b. The FFQ-1, which takes into account the process dynamics, shows deviations from the minimum reboiler duty and the target $NH_3$ concentration because the transfer function $G_f$ was determined using the average of the operation results at high and low $NH_3$ concentration levels of SSW. On the response of $X_{SSW,NH_3}$, the FFQ-2 gives very slow response because of the lack of consideration of process dynamics. Furthermore, because the very low $NH_3$ concentration of the SSW, it is very sensitive to the small change of reboiler duty. This effect is shown in the small deviation of the target reboiler duty from the true minimal value and the relative large deviation of $NH_3$ concentration from the target of 20 ppmw. Although the process dynamics were not considered in FFT either, the response of $X_{SSW,NH_3}$ is fast and meets the target value of 20 ppmw. The superior performance of FFT comes from the appropriateness of the stage 29 for inferential control and the prompt effect of adjusting reboiler duty based on the stage 29 temperature.

The responses of feedback control schemes to −10% feed flow rate change are shown in Figure 8c,d. The responses of the feedback control of $X_{SSW,NH_3}$ with 3, 10, and 20 min time delay of concentration measurement, i.e., FBA-DT3, -DT10, and -DT20, are similar. The longer the measurement delay, the longer the settling time. An important feature is the integration windup problem, as shown in Figure 8d, where the concentration remains at near zero level for very long time before starting to increase and the problem is more severe when the measurement delay is longer. This issue causes the need for over reduction of reboiler duty and results in the overshooting of concentration after the windup period. The problem can be solved by adopting the external reset feedback control scheme, FB-ER-DT3, -DT10, and -DT20, and the corresponding responses are shown in Figure 8e,f. In addition to the shortening of the settling time, significant reduction of reboiler duty can be obtained. The performance of the cascade feedback control scheme FBAT is much better than all the other feedback control schemes discussed above, as shown in Figure 8c,d. Note that in the FBAT scheme, the measurement lag is 20 min. However, because the optimal temperature of stage 29 does not vary significantly with the feed stream flowrate change, fast response can be obtained.

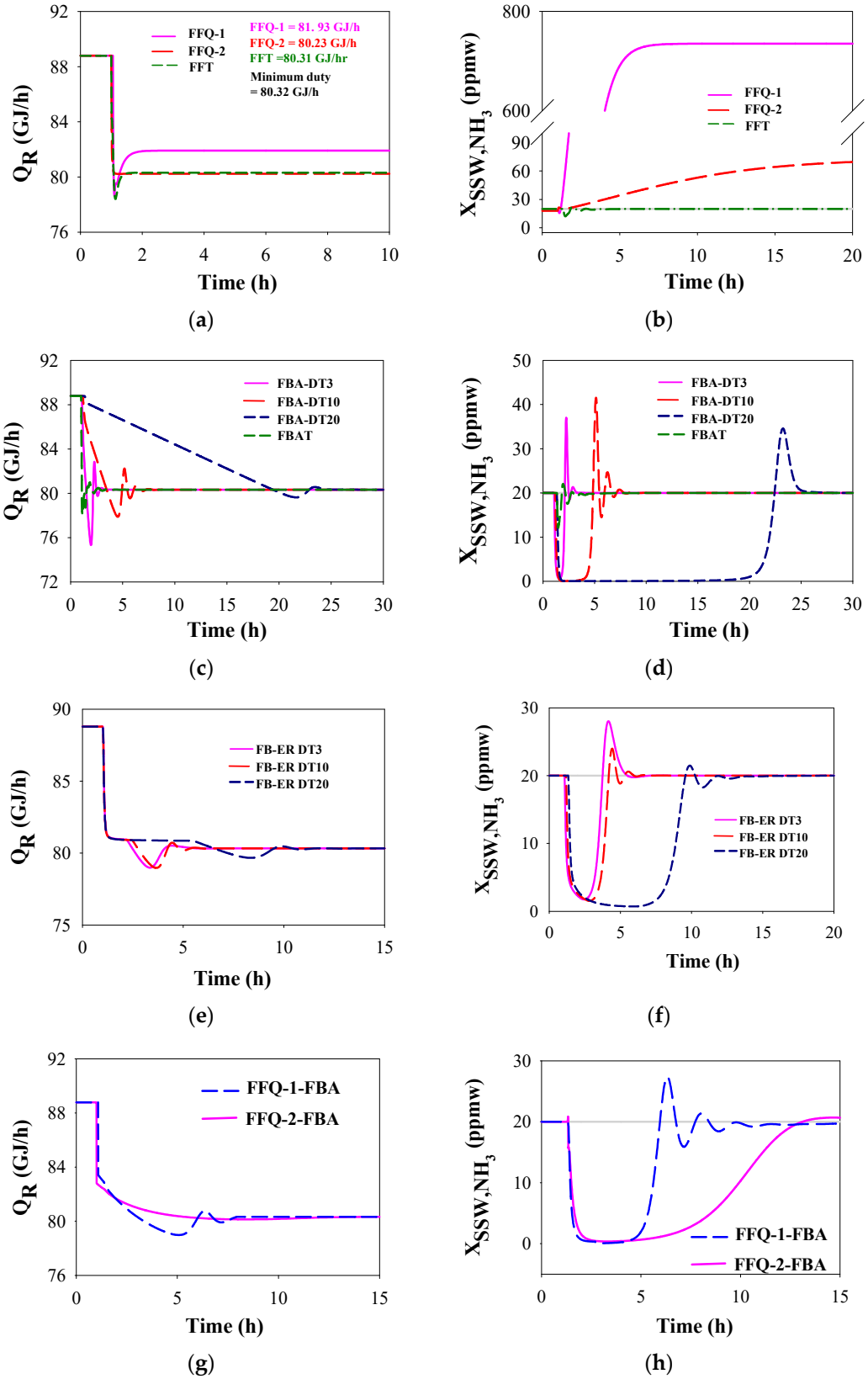


**Figure 8.** The dynamic responses (reboiler duty and stripped sour water (SSW) $NH_3$ concentration) of the sour water stripper (SWS) employing different control schemes to the sour water feed flowrate disturbance with −10% change, (**a**,**b**) for feedforward control, (**c**–**f**) for feedback control, (**g**,**h**) for feedforward-feedback control.

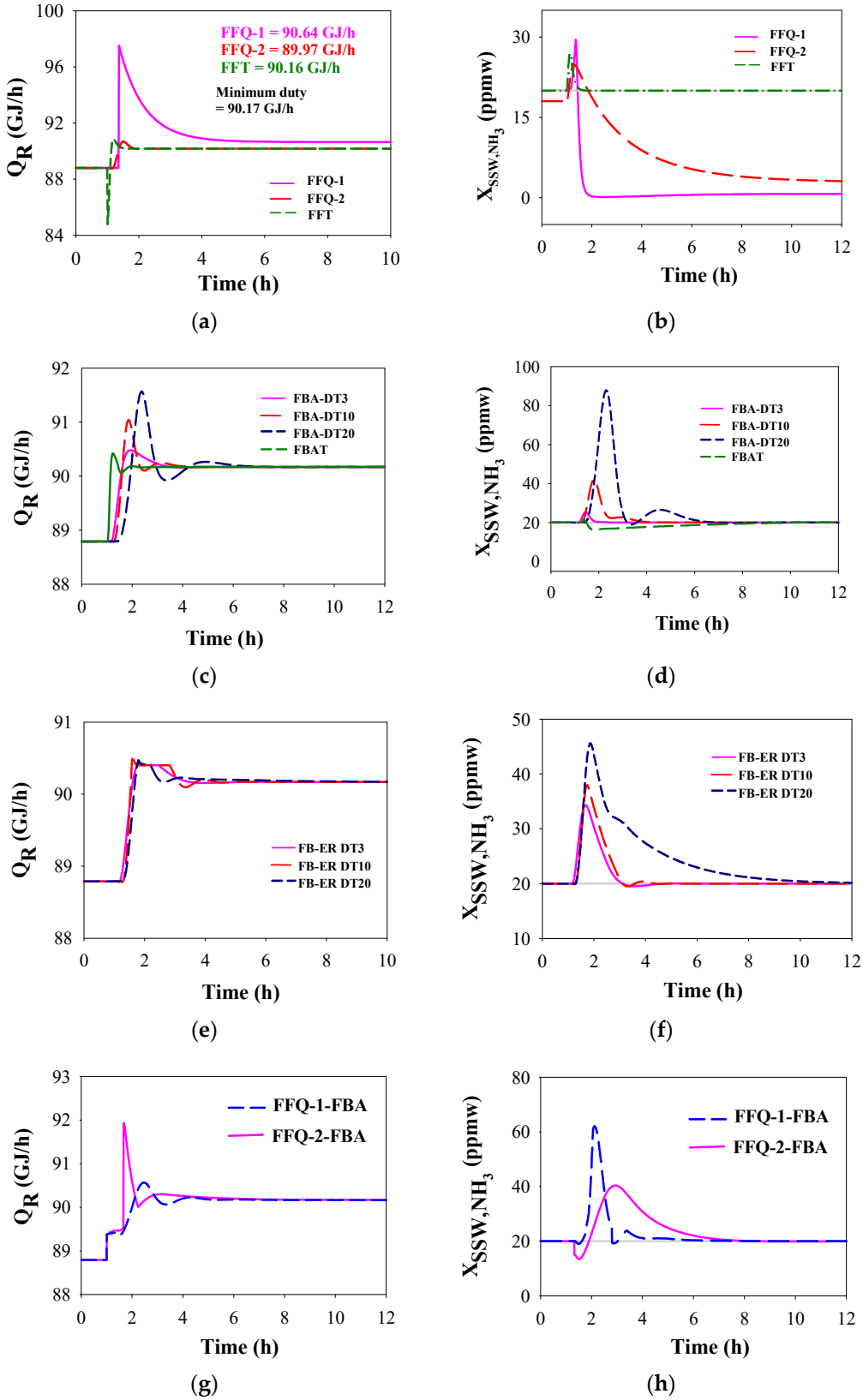


**Figure 9.** The dynamic responses (reboiler duty and SSW $NH_3$ concentration) of the SWS employing different control schemes to the sour water feed $NH_3$ concentration disturbance with +10% change, (**a**,**b**) for feedforward control, (**c**–**f**) for feedback control, (**g**,**h**) for feedforward-feedback control.

The responses of feedforward-feedback control schemes to −10% feed flow rate change are shown in Figure 8g,h. The feedback control scheme FBA-DT20 is integrated with FFQ-1 and FFQ-2. The deviations of final reboiler duty and $NH_3$ concentration values from their target values occur in FFQ-1 and FFQ-2 can be eliminated by the control action provided by the feedback loop FBA. Compared to FFQ-2, FFQ-1 gives faster response due to its inclusion of process dynamics.

For the +10% change of $NH_3$ concentration disturbance, the control responses shown in Figure 9 are similar to Figure 8 except the direction and extent of change of the reboiler duty and $NH_3$ concentration of SSW are different. For the FBA control scheme, the integration windup problem does not occur. However, the adoption of external reset feedback still provides better response in terms of lower $NH_3$ concentration and reboiler duty as shown in Figure 9c–f. Unlike the response to the flowrate disturbance discussed above, the response of FBAT to the $NH_3$ concentration disturbance shows greater influence from the long measurement delay of 20 min as can be observed in Figure 9d in terms of longer time to meet the setpoint value.

### *4.2. Performance Index*

#### 4.2.1. Settling Time

The time needed for the controlled variable, i.e., the $NH_3$ concentration of the SSW, to stabilize with fluctuation between ±1% of the final steady state value is defined as the settling time. The settling time shown in Figure 10 is the average of the settling times of the +10% and −10% disturbance changes. The results indicate that for the SWS with the most basic control scheme with long measurement delay, that is FBA-DT20, the settling time can be more than 27 h. However, if the measurement delay is short, such as the FBA-DT3, the settling time can be reduced to about 3 h. The settling time of FFT is close to FBA-DT3. However, the final steady state values of FFT and the other two feedforward control schemes, FFQ-1 and FFQ-2, cannot meet the target value. Compared to the basic feedback control, FBA, the alternative control schemes, including feedforward, feedback with external reset, and feedforward-feedback, do not provide significant reduction of the settling time except the FFT.

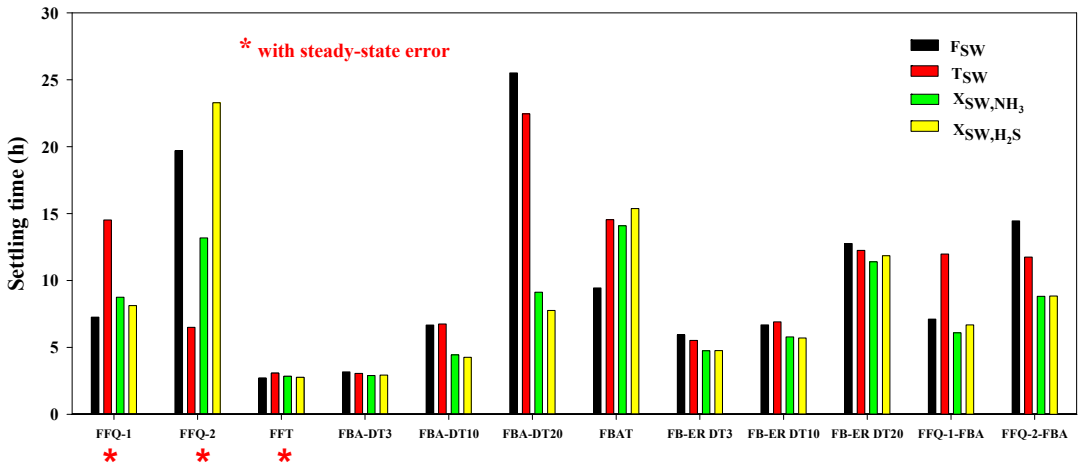


**Figure 10.** Settling time results of all control schemes for the sour water feed stream disturbances, including flowrate, temperature, $NH_3$ concentration, and $H_2S$ concentration. (* with steady state offset).

#### 4.2.2. Integrated Absolute Error of Ammonia Concentration

The integrated absolute error (IAE) of the $NH_3$ concentration of the SSW is defined as:

$$IAE_{NH_3} = \int_{t_{initial}}^{t_{final}} \left| X_{SWS,NH_3} - X_{SWS,NH_3,target} \right| dt \quad (6)$$

where the target concentration is 20 ppmw and the integration is from the initial time of the disturbance change to the final settling time. The result shown in Figure 11 is the average of the +10% and −10% disturbance changes.

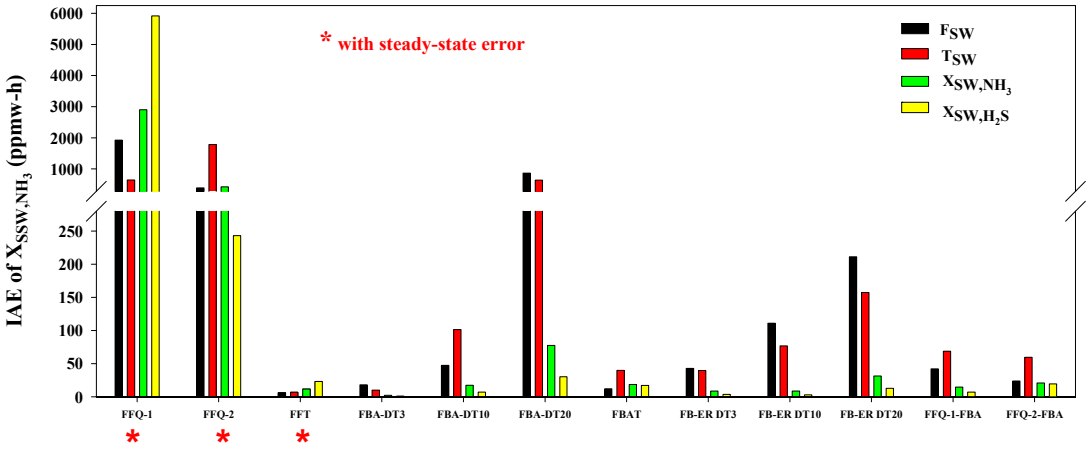


**Figure 11.** Integrated absolute error (IAE) of $NH_3$ concentration results of all control schemes for the sour water feed stream disturbances, including flowrate, temperature, $NH_3$ concentration, and $H_2S$ concentration. (* with steady state offset).

The control schemes with high $IAE_{NH_3}$ value are FFQ-1, FFQ-2, FBA-DT20, and FB-EF-DT20 due to the substantial steady state offset and the long measurement delay. The control schemes with the lowest $IAE_{NH_3}$ value are FFT and FBA-DT3. Note that the steady state offset of FFT is small. The FB-ER control schemes do not provide significant improvement in $IAE_{NH_3}$ compared to their FBA counterpart control schemes. FBAT, FFQ-1-FBA, and FFQ-2-FBA are the next best control schemes.

#### 4.2.3. Integrated Absolute Error of Specific Reboiler Duty

The integrated absolute error (IAE) of the specific reboiler duty is defined as:

$$IAE_{\overline{Q}_R} = \int_{t_{initial}}^{t_{final}} \left| \overline{Q}_R - \overline{Q}_{R,target} \right| dt \quad (7)$$

where the specific reboiler duty is the reboiler duty per unit sour water feed flowrate. While the target specific reboiler duty is the minimum reboiler duty required to meet the SSW $NH_3$ concentration limit of 20 ppmw. The integration is from the initial time of the disturbance change to the final settling time. The result shown in Figure 12 is the average of the +10% and −10% disturbance changes.

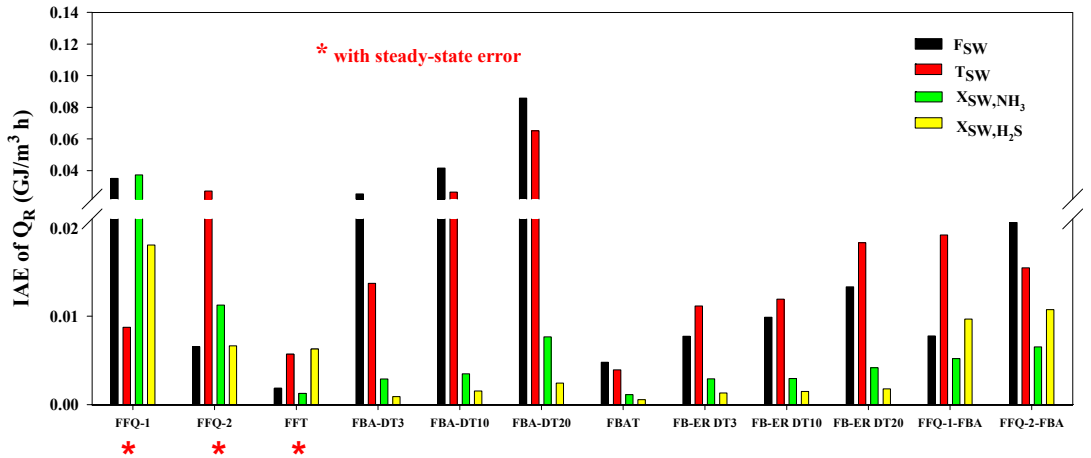


**Figure 12.** IAE of specific reboiler duty results of all control schemes for the sour water feed stream disturbances, including flowrate, temperature, $NH_3$ concentration, and $H_2S$ concentration. (* with steady state offset).

The control schemes that give the lowest $IAE_{\overline{Q}_R}$ value are FBAT and FFT and the ones with the highest values are FBA control schemes. The extent of improvement in $IAE_{\overline{Q}_R}$, relative to the FBA control schemes, is feedback with external reset > feedforward-feedback > feedforward.

## 5. Conclusions

For the sour water stripper in petroleum refining, this study developed estimators for the $NH_3$ and $H_2S$ concentrations in the sour water feed stream based on the properties that can be online measured conveniently. These estimators assist the function of feedforward control for instant reacting to the disturbances of feed stream.

Various control schemes based on feedforward, feedback, feedback with external reset, and feedforward-feedback structures were developed. The dynamic responses of all the control schemes to the disturbances of the sour water feed stream, including the flowrate, temperature, $NH_3$ concentration, and $H_2S$ concentration, were obtained from the rigorous dynamic simulation model of the sour water stripper. Quantitative performance comparison in terms of settling time, IAE of $NH_3$ concentration of the stripped sour water, and IAE of specific reboiler duty reveals that

- FFT and FBA-DT3 are the best control schemes considering all three performance indices.
- FBAT is the next best choice with slightly worse performance in settling time.
- FFT must be implemented with the feed concentration estimators and its final steady state value might exhibit small deviation from the target setpoint.

This study is based on the first principles simulation models of the sour water stripper. Hence, the effects of model mismatch with the real plant operation and the noise or measurement errors are not taken into account.

**Author Contributions:** Conceptualization, Y.-H.C.; Formal analysis, Y.-H.C.; Funding acquisition, C.-D.H.; Investigation, Y.-H.C., H.C.; Methodology, Y.-H.C.; Project administration, C.-D.H.; Software, C.-M.C.; Visualization, C.-M.C.; Writing—original draft, Y.-H.C.; Writing—review and editing, H.C. All authors have read and agreed to the published version of the manuscript.

**Funding:** This research was funded by the Ministry of Science and Technology of Taiwan, grant number MOST 109-2221-E-032-013.

**Conflicts of Interest:** The authors declare no conflict of interest.

## Abbreviations

| | |
|---|---|
| A | Composition |
| D | Diameter (m) |
| DT | Measurement time delay (min) |
| ER | External reset |
| F | Flow rate ($m^3/h$) |
| FB | Feedback |
| FF | Feedforward |
| G | Transfer function |
| H | Height (m) |
| IAE | Integrated absolute error |
| K | Gain (%/%) |
| ORC | Override controller |
| pH | pH value (-) |
| Q | Heat duty (GJ/h) |
| $\overline{Q}_R$ | Specific reboiler duty ($GJ/m^3$) |
| $R^2$ | Coefficient of determination |
| SSW | Stripped sour water |

| | |
|---|---|
| SWS | Sour water stripper |
| T | Temperature (°C) |
| X | Mass fraction |
| Greek symbol | |
| $\alpha$ | Dead time (h) |
| $\beta$ | Lead time (h) |
| $\theta$ | Dead time (h) |
| $\varrho$ | Density (kg/m$^3$) |
| $\tau$ | Time constant (h) |
| Subscript | |
| d | Disturbance |
| f | Feedforward |
| p | Process |
| R | Reboiler |
| SW | Sour water |

## References


1. Sun, P.; Elgowainy, A.; Wang, M.; Han, J.; Henderson, R.J. Estimation of U.S. refinery water consumption and allocation to refinery products. *Fuel* **2018**, *221*, 542–557. [CrossRef]
2. Das, S.; Singh, N.K. Configuration study and design of sour water stripper units for a refinery revamp. *Hydrocarb. Process.* **2018**, *5*, 89–93.
3. Weiland, R.H.; Hatcher, N.A. Sour water strippers exposed. In Proceedings of the Laurence Reid Gas Conditioning Conference, Norman, OK, USA, 28 February 2012.
4. Lieberman, N. Sour Water Strippers: Design and Operation. 2013. Available online: www.digitalrefining.com/article/1000799 (accessed on 22 July 2020).
5. Kazemi, A.; Mehrabani-Zeinabad, A.; Beheshti, M. Development of a novel processing system for efficient sour water stripping. *Energy* **2017**, *125*, 449–458. [CrossRef]
6. Zahid, U. Techno-economic evaluation and design development of sour water stripping system in the refineries. *J. Clean. Prod.* **2019**, *236*, 117633. [CrossRef]
7. Gai, H.; Chen, S.; Lin, K.; Zhang, X.; Wang, C.; Xiao, M.; Huang, T.; Song, H. Conceptual design of energy-saving stripping process for industrial sour water. *Chin. J. Chem. Eng.* **2020**, *28*, 1277–1284. [CrossRef]
8. Armstrong, T. Optimize sour water treatment. *Hydrocarb. Process.* **2003**, *6*, 77–79.
9. Graziani, S.; Xibilia, M.G. A deep learning based soft sensor for a sour water stripping plant. In Proceedings of the 2017 IEEE International Instrumentation and Measurement Technology Conference, Turin, Italy, 22–25 May 2017.
10. Barros, D.J.S.; Barros, E.S.; Zanoelo, E.F. Soft-sensor models to estimate the efficiency of $H_2S$ removal from an oil refinery stream of nonphenolic sour water. *Chem. Eng. Commun.* **2018**, *205*, 1050–1059. [CrossRef]
11. Bellen, J. Design of sour water stripping system. In Proceedings of the 70th Philippine Institute of Chemical Engineers Annual National Convention, Davao City, Philippine, 25–27 February 2009.
12. Morado, H.P.M.C.; de Medeiros, J.L.; Araújo, O.Q.F. Emission minimization of a two-stage sour water stripping unit using surrogate models for improving heat duty control. *J. Sustain. Dev. Energy Water Environ.* **2019**, *7*, 305–324. [CrossRef]
13. Aspen Technology. *Aspen Plus® V10*; Aspen Technology Inc.: Bedford, UK, 2018.
14. Newman, S.A. Sour water design by charts. *Hydrocarb. Process.* **1991**, *70*, 145–150.
15. Montgomery, D.C. *Design and Analysis of Experiments*, 9th ed.; John Wiley & Sons: New York, NY, USA, 2017.
16. Seborg, D.E.; Edgar, T.F.; Mellichamp, D.A.; Doyle, F.J. *Process Dynamics and Control*, 4th ed.; John Wiley & Sons: Hoboken, NJ, USA, 2017.
17. Luyben, W.L. *Plantwide Dynamic Simulators in Chemical Processing and Control*; Taylor & Francis: Abingdon, UK, 2002.
18. Ziegler, J.G.; Nichols, N.B. Optimum settings for automatic controllers. *Trans. ASME* **1942**, *64*, 759–768. [CrossRef]
19. Shinskey, F.G. *Process Control Systems*, 4th ed.; McGraw-Hill: New York, NY, USA, 1996.
20. Luyben, W.L. *Distillation Design and Control Using AspenTM Simulation*, 2nd ed.; John Wiley & Sons: Hoboken, NJ, USA, 2013.